Journal of Power Sources 194 (2009) 805–810

Contents lists available at ScienceDirect

Journal of Power Sources

journal homepage: www.elsevier.com/locate/jpowsour

Short communication

High-performance core–shell PdPt@Pt/C catalysts via decorating PdPt alloy cores with Pt

Yan-Ni Wu [a,b], Shi-Jun Liao [a,*], Zhen-Xing Liang [a], Li-Jun Yang [a], Rong-Fang Wang [a]

[a] School of Chemistry and Chemical Engineering, South China University of Technology, Guangdong, Guangzhou 510640, China
[b] School of Chemistry and Chemical Engineering, Zhao Qing University, Guangdong, Zhao Qing 526061, China

ARTICLE INFO

Article history:
Received 1 May 2009
Received in revised form 19 June 2009
Accepted 19 June 2009
Available online 30 June 2009

Keywords:
Electrocatalyst
Fuel cells
Low-platinum catalyst
Methanol oxidation
Oxygen reduction

ABSTRACT

A core–shell structured low-Pt catalyst, PdPt@Pt/C, with high performance towards both methanol anodic oxidation and oxygen cathodic reduction, as well as in a single hydrogen/air fuel cell, is prepared by a novel two-step colloidal approach. For the anodic oxidation of methanol, the catalyst shows three times higher activity than commercial Tanaka 50 wt% Pt/C catalyst; furthermore, the ratio of forward current I_f to backward current I_b is high up to 1.04, whereas for general platinum catalysts the ratio is only ca. 0.70, indicating that this PdPt@Pt/C catalyst has high activity towards methanol anodic oxidation and good tolerance to the intermediates of methanol oxidation. The catalyst is characterized by X-ray diffraction (XRD), transmission electron microscopy (TEM), and X-ray photoelectron spectroscopy (XPS). The core–shell structure of the catalyst is revealed by XRD and TEM, and is also supported by underpotential deposition of hydrogen (UPDH). The high performance of the PdPt@Pt/C catalyst may make it a promising and competitive low-Pt catalyst for hydrogen fueled polymer electrolyte membrane fuel cell (PEMFC) or direct methanol fuel cell (DMFC) applications.

1. Introduction

Platinum-based catalysts have been widely acknowledged as the best active catalytic components for low-temperature fuel cells, including the hydrogen fueled polymer electrolyte membrane fuel cell (PEMFC) and the direct alcohol fuel cell (DAFC). However, platinum is a rare and precious metal, and its limited availability and high price are the two most important factors impeding the commercialization of low-temperature fuel cells. Reducing platinum use has thus become a critical focus of fuel cell research [1,2].

Although major progress has been made in developing non-platinum catalysts [3–8], the relatively low electrocatalytic activity and stability of such catalysts make their use in low-temperature fuel cells problematic, at least in the near future. Thus, it is desirable to develop low-Pt-content catalysts to improve utilization of the noble metal and thereby reduce the amount used in fuel cell electrodes.

Preparation of a core–shell structure catalyst, in which the active metal (e.g., Pt) is only distributed on the surface of a core composed of a transition metal other than Pt, is doubtless an attractive approach because it offers the possibility of increasing Pt utilization and thus lowering Pt loading. A few attempts have been reported recently. Lim et al. synthesized Pd–Pt bimetallic nanodendrites consisting of a dense array of Pt branches on a Pd core; on the basis of equivalent Pt mass, these were two and a half times more active for the ORR than a state-of-the-art Pt/C catalyst [9]. Adzic et al., for example, reported the preparation of an ORR electrocatalyst, consisting of Pt and another late transition metal (M, where M = Ir, Ru, Rh, Pd, Au, Re, or Os) deposited as a monolayer on the surfaces of Pd single crystals or carbon-supported Pd nanoparticles, using an underpotential deposition of metal method; these catalysts achieved a very high activity for oxygen reduction compared to pure Pt ORR catalyst. Although they did not describe their catalyst as having a core–shell structure, it clearly had the characteristics of core–shell catalysts [10]. They also reported a low-platinum catalyst that had platinum deposited on the surface of gold nanoparticles [11].

In recent years, a Pt@Au/C catalyst was investigated and reported by a few groups. For example, Kristian et al. used a reduction strategy to synthesize a Pt_{shell}–Au_{core}/C electrocatalyst that had a higher specific activity than the conventional Pt/C catalyst towards the methanol oxidation reaction [12].

In this paper, a core–shell PdPt@Pt/C catalyst was successfully synthesized using a high-pressure colloidal method: we first prepared the carbon-supported alloy metal catalyst PtPd/C, then deposited a platinum layer on the supported PtPd nanoparticles. To obtain high dispersion, we used a PtPd alloy particle rather than a pure Pd nanoparticle as the core pure Pd nanoparticle aggregates easily. Interestingly, the PdPt@Pt/C catalyst showed particularly

* Corresponding author. Tel.: +86 20 8711 3586; fax: +86 20 8711 3586.
E-mail address: chsjliao@scut.edu.cn (S.-J. Liao).

0378-7753/$ – see front matter © 2009 Elsevier B.V. All rights reserved.
doi:10.1016/j.jpowsour.2009.06.069

high activity for both anodic methanol oxidation and cathodic oxygen reduction.

2. Experimental

The carbon-supported PdPt alloy cores were prepared by an organic colloid method [2]; palladium chloride ($PdCl_2$) and sodium citrate were dissolved in ethylene glycol (EG) and then stirred for 30 min. Afterwards, hexachloroplatinate acid and sodium citrate were added. After another 30 min of stirring, Vulcan XC72 carbon black (Cabot Corp., BET: 237 $m^2\ g^{-1}$, denoted as C) was then added to the mixture (metal loading: 23 wt% and atomic ratio Pd:Pt = 3:1) under stirred conditions. The pH of the solution was adjusted to >10 by the drop-wise addition of a 5 wt% KOH/EG solution, under vigorous stirring. The mixture was then placed into a Teflon®-lined autoclave and conditioned at 160 °C for 8 h, followed by filtering, washing and vacuum drying at 90 °C. Then the PdPt@Pt/C catalyst was prepared by depositing a shell platinum layer on the surface of the PdPt/C prepared in step 1; the method and procedures were similar to those in step 1 except that no palladium chloride was added. The total metal loading was ca. 23 wt% and the nominal Pt content was ca. 8 wt%. For comparison, the 20 wt% Pd/C, Pt/C, and PdPt/C catalysts were prepared using the same approach.

The morphologies of the prepared catalysts were observed using scanning transmission electron microscopy (Hitachi HD-2000 STEM) at 200 kV, and using transmission electron microscopy (JEOL JEM-2010HR, Japan).

X-ray diffraction (XRD) analysis was performed using a Shimadzu XD-3A (Japan) X-ray diffractometer with a filtered Cu Kα radiation source, operated at 35 kV and 30 mA. Diffraction patterns were collected from 20° to 80° at a scanning rate of 4° min^{-1}, and with a step size of 0.01°.

The electrochemical reactivity of the catalyst was measured by cyclic voltammetry (CV) using a three-electrode cell in an IM6e electrochemical work station (Zahner, Germany) at room temperature. A platinum wire and an Ag/AgCl electrode were used as the counter and reference electrodes, respectively. The working electrode was a glassy carbon disk (5 mm in diameter) covered with a thin layer of Nafion®-impregnated catalyst. The thin-film electrode was prepared as follows: 5 mg of catalyst was dispersed in 1 mL Nafion®/ethanol (0.25% Nafion®) by sonication for 20 min, and 4 μL of the dispersion was transferred onto the glassy carbon disk using a pipette. A CV test was conducted at 50 mV s^{-1} in a solution of 0.5 M H_2SO_4 or 0.5 M H_2SO_4 with 0.5 M CH_3OH, in the potential range of −0.2 to 1.0 V. The Pt loadings of the Pt/C and PdPt@Pt/C catalysts on the electrode surface were 0.0200 and 0.0082 mg Pt cm^{-2}, respectively.

The X-ray photoelectron spectroscopy (XPS) measurement was performed on a Perkin Elmer PHI1600 system (PerkinElmer, USA) using a single Mg Kα X-ray source operating at 300 W and 15 kV of voltage.

TPR measurement was carried out in an AutoChem II 2920 characterization system (Micromeritics, USA) from room temperature to 600 °C with an increase rate of 5 °C min^{-1}. Prior to measurement, the sample was purged for 30 min at room temperature in an argon stream with a flow rate of 30 mL min^{-1}.

3. Results and discussion

3.1. Catalyst morphology

It is difficult to observe the core–shell structure of PdPt@Pt/C directly by TEM, because the particles are too small, the platinum layer is too thin, platinum and palladium have almost the same

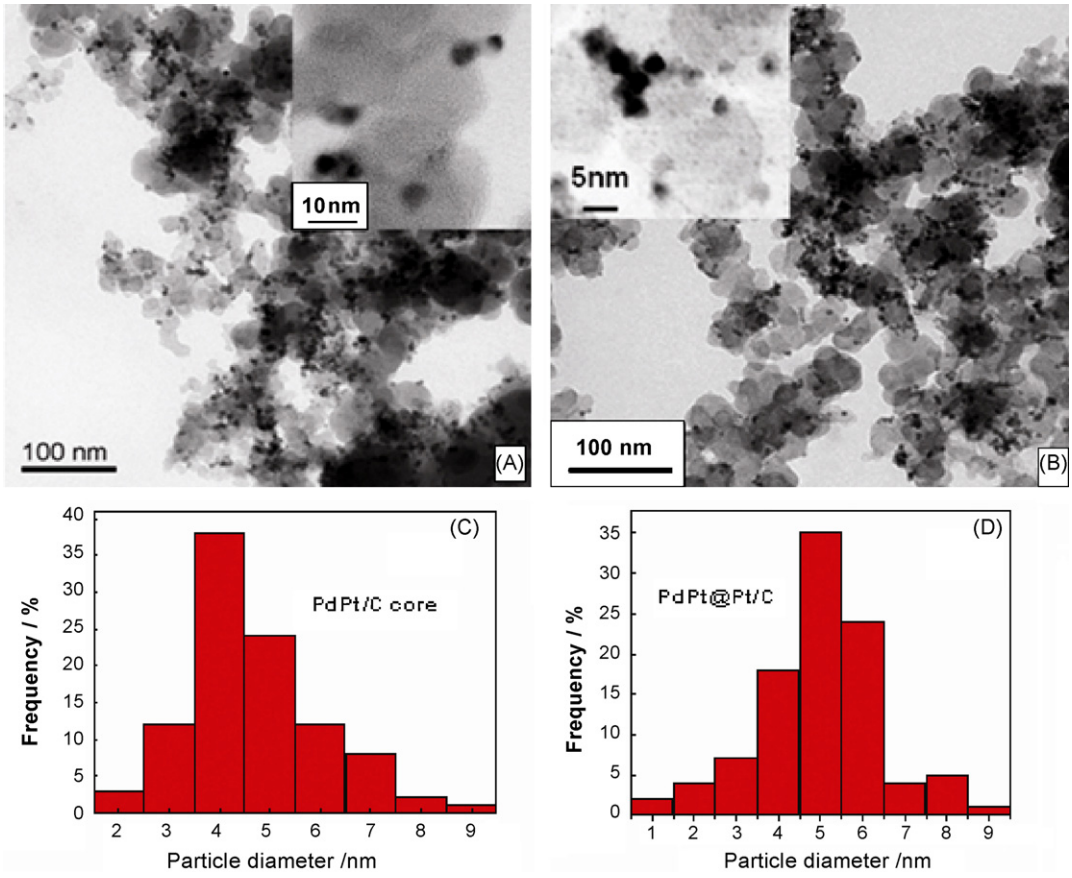

Fig. 1. TEM images of the PdPt/C (core) (A) and PdPt@Pt/C (B) samples; histogram of the size distribution of the PdPt/C (core) (C) and PdPt@Pt/C (D).

crystal structure and characteristics, and the PtPd and PtPd@Pt particles were not well crystallized. But the TEM measurements give some important information for this catalyst. Fig. 1A and B shows TEM images of the PdPt@Pt/C catalyst and its precursor core, PtPd/C. It can be seen that the active components are highly dispersed on the carbon supports, with a narrow size distribution (Fig. 1C and D), the average crystallite sizes being ca. 4.4 and 4.8 nm for PtPd/C and PtPd@Pt/C, respectively. We think the slight increase in particle size may result from the coverage of platinum on the PtPd core nanoparticles; in other words, it can be viewed as confirming the core–shell structure of the PtPd@Pt/C catalyst.

The particle size of PtPd/C is markedly larger than that of the Pt/C or Pd/C catalysts we have previously reported, which was prepared by the same method and under almost the same conditions. The reason for this difference is palladium's strong tendency to aggregate. When we tried to prepare a pure palladium core material, Pd/C, we found that the aggregation was too great to obtain high dispersion of the Pd/C materials, so we chose instead to use a PtPd alloy particle as the core for preparing the catalyst.

It is also clear that the distribution density of the active component particles in PdPt@Pt is almost the same as, but not higher than, that in PtPd/C (see Fig. 1A and B), which implies that most of the platinum was reduced and deposited on the outside of the PdPt particles, instead of independent platinum particles being generated on the carbon support. It is reasonable to suggest that the platinum would be preferentially reduced and then cover the PdPt particles, because the interaction between the metals would be stronger than that between metal and carbon. The core–shell structure of PtPd@Pt/C, or the fact that platinum covered the outside of the PdPt-core nanoparticles, can be supported by the following XRD, XPS, TPR, and UPDH results.

Fig. 2 shows the XPS spectra of PdPt/C and PtPd@Pt/C. The platinum peak in PtPd@Pt/C is obviously stronger than the peak in PtPd/C (see Fig. 2A and B). The atom ratio of Pt to Pd is 0.7 in PtPd@Pt/C, but only 0.2 in the PtPd/C core material, indicating that platinum covered the surface of the PtPd/C particles and enhanced the surface content of platinum in PtPd@Pt/C; these findings strongly support the suggestion that the PtPd@Pt/C catalyst has a core–shell structure.

Fig. 2C and D shows the XPS spectra of Pt 4f in PtPd@Pt/C and PtPd/C, respectively; the binding energy of the Pt (0) $4f_{7/2}$ peak in PdPt@Pt/C is a little bit higher (0.24 eV) than that in PdPt/C. This shift was also reported by Zhou et al. in their prepared core–shell Au@Pd catalyst [13]. The binding energy shift may be attributed to the interaction between the two metals in the PtPd@Pt/C catalyst.

Fig. 3A shows XRD patterns for PtPd/C and PtPd@Pt/C; all of the peaks for PtPd@Pt/C are clearly stronger than those of PtPd/C, due to the platinum on the surface of the PtPd particles. The particle sizes, calculated from XRD data by Jade software, were 4.2 and 4.5 nm, respectively, the size increase before and after Pt deposition confirming that platinum decorated the surface of the PtPd particles in the second preparation step. The thickness of the shell layer was ca. 0.15 nm.

It is interesting to note that the diffraction peak (2 2 0) for the PdPt@Pt/C catalyst is between those of Pt/C and Pd/C (see the inset in Fig. 3B), and that it has a small positive shift compared to pure Pt/C, and a small negative shift compared to Pd/C.

The lattice parameters of the catalysts are calculated and listed in Table 1. It can be seen that the lattice parameter of the PdPt@Pt/C

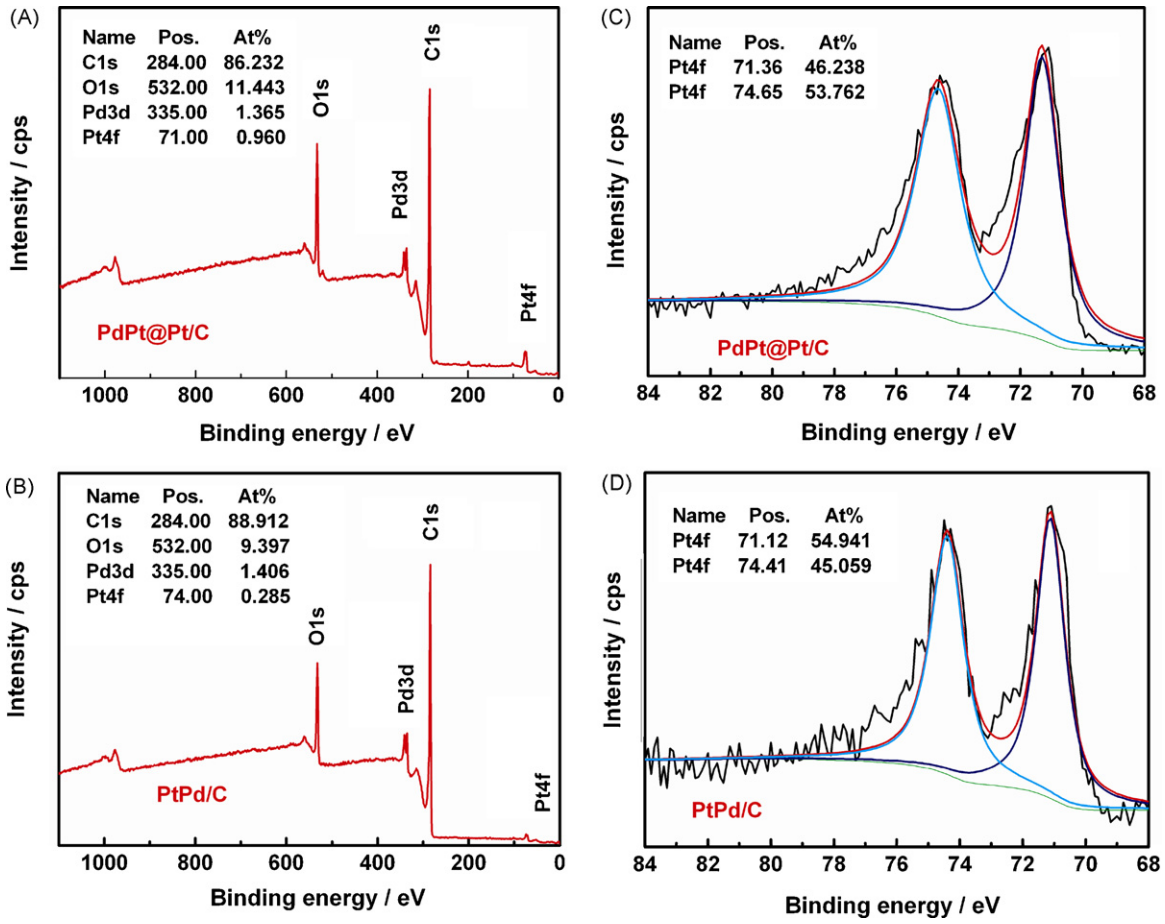

Fig. 2. XPS survey scans of the PdPt@Pt/C (A) and PtPd/C (B), the Pt 4f core level XPS spectra of the catalysts PdPt@Pt/C (C) and PtPd/C (D).

Table 1
Lattice parameters of the 20 wt% Pt/C, Pd/C, and PdPt@Pt/C catalysts.

Sample 20 wt% metal	XRD crystallite size[a] (nm)	Pt (wt%)	M–M bond distance (nm)	Lattice parameter (nm)
Pt/C	2.1	20	0.2778	0.3982
Pd/C	3.8	0	0.2750	0.3889
PdPt@Pt/C	4.5	8	0.2770	0.3927

[a] Particle size is estimated from XRD patterns.

catalyst is larger than that of pure Pd but smaller than that of pure Pt, implying an interaction between Pt and Pd in the cores and between the cores and shells. It may be that an alloy of Pt and Pd was formed in the PdPt cores, a possibility that is supported by TPR results, as shown in Fig. 4. There, the reduction peak temperature of the carbon-supported PtPd precursor is lower than that of the carbon-supported platinum precursor and higher than that of the carbon-supported palladium precursor.

To understand the core–shell structure of PtPd@Pt/C catalyst, a series of catalysts were investigated by cyclic voltammetry in sulfuric solution, as this can be regarded as a surface-sensitive technique that detects the electrochemical properties of surface atoms only, rather than of bulk atoms [14]. As shown in Fig. 5, for the Pd/C catalyst, a very strong hydrogen oxidation peak can be observed, which is attributable to the strong hydrogen storage property of Pd, but for the PtPd/C sample we used as the core, this hydrogen peak was

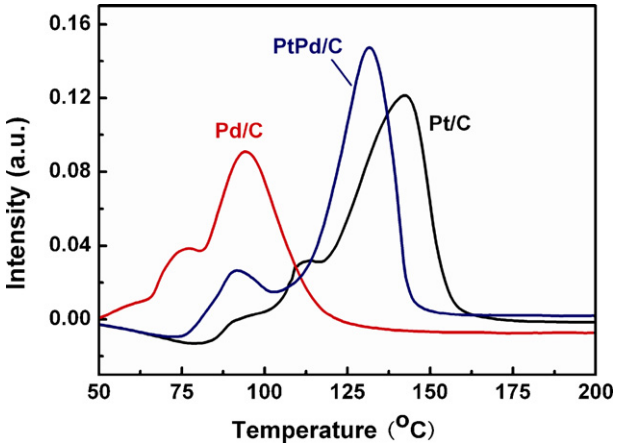

Fig. 4. TPR profiles of Pt/C, Pd/C, and PtPd/C catalysts.

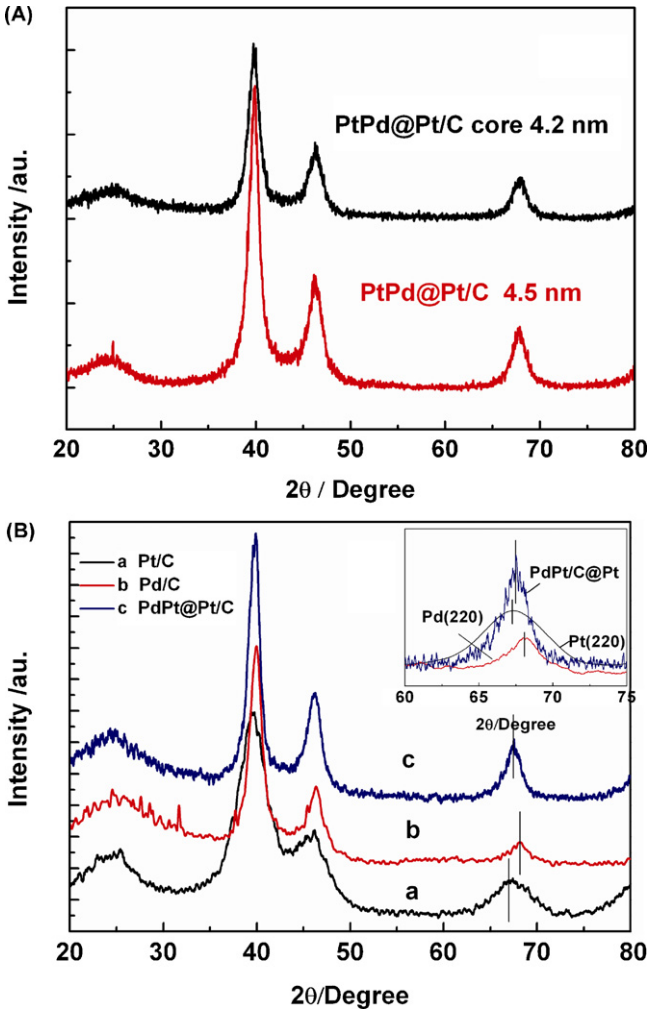

Fig. 3. (A) XRD patterns of PtPd/C and PtPd@Pt/C; (B) comparison of XRD patterns of Pt/C (a), Pd/C (b), and PdPt@Pt/C (c).

sharply reduced due to the addition of platinum. As expected, the typical double peak can be observed for the Pt/C catalyst.

From Fig. 5, we can see that the hydrogen oxidation peak of the PtPd@Pt/C catalyst is close to that of Pt/C, with virtually no hydrogen peak in the region where a large peak appears for Pd/C; however, the new feature of one big broad peak does not exhibit the typical two or three peaks of pure polycrystalline Pt/C, which are associated with weakly and strongly bonded hydrogen species on different crystal faces of Pt metal. The PtPd@Pt/C peak looks much more like that of the Pt alloy catalyst than that of the Pd/C catalyst. The absence of Pd features and of the typical two or three resolved peaks in the hydrogen adsorption–desorption region of Pt implies that all or most of the PtPd core surfaces had already been covered by Pt shells, and that an interaction occurred between the palladium in the cores and the platinum in the shell layers. Thus, the core–shell

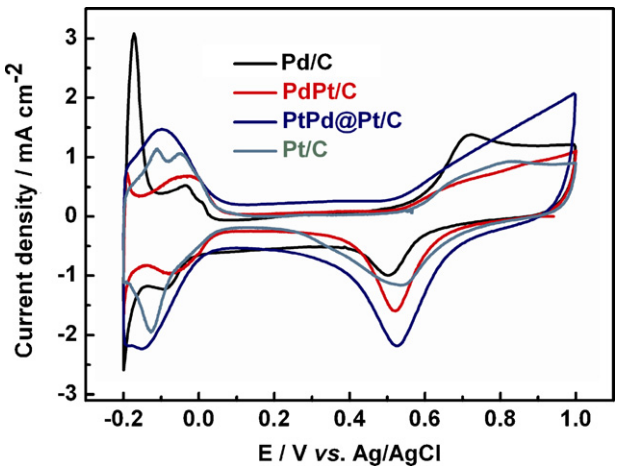

Fig. 5. Cyclic voltammograms of Pd/C, PdPt/C, PdPt@Pt/C, and Pt/C catalyst electrodes measured in N_2-purged 0.5 M H_2SO_4 electrolyte, at room temperature and with a sweep rate of 50 mV s^{-1}.

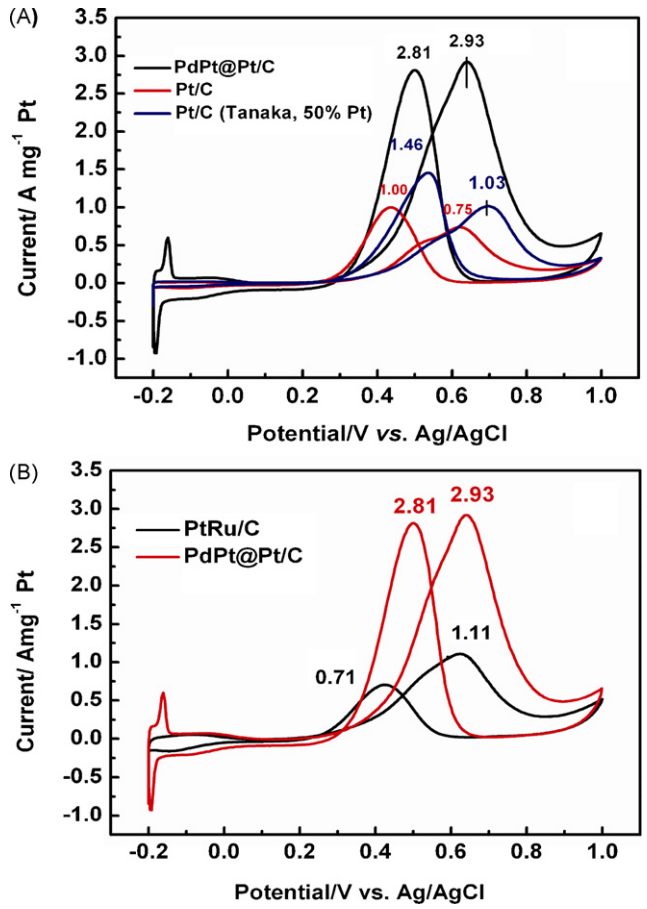

Fig. 6. (A) Cyclic voltammograms of Pt/C, PdPt@Pt/C, and Tanaka 50 wt% Pt/C in 0.5 M H_2SO_4 + 0.5 M CH_3OH at room temperature; metal loadings 0.02 mg cm^{-2}, sweep rate 50 mV s^{-1}, and rotating rate 300 rpm. (B) Cyclic voltammograms of 20 wt% PtRu/C (Pt 13%, Ru7%; Pt loading 0.014 mg Pt cm^{-2}, Ru loading 0.007 mg Pt cm^{-2}), PdPt@Pt/C and Pd/C under same conditions as (A).

structure, or the coverage of platinum on the surface of PtPd cores in PtPd@Pt/C, was confirmed by CV in 0.5 M H_2SO_4 solution.

Furthermore, the electrochemical active area (EAA) of the PtPd@Pt/C was high, up to 301.6 m^2 g^{-1} Pt, which was 6% higher that that of the Pt/C (285.1 m^2 g^{-1}), this result revealed that the platinum was highly dispersed in the core–shell structure catalyst.

Put simply, the core–shell structure of the PdPt@Pt/C catalyst was strongly confirmed or supported by XPS, XRD, and hydrogen desorption/adsorption, even though this structure could not be observed directly by TEM.

3.2. The activity of PtPd@Pt/C for anodic methanol oxidation and oxygen reduction

It is exciting that the core–shell PtPd@Pt/C catalyst exhibited very high activity towards the anodic oxidation of methanol, as well as the reduction of oxygen.

As shown in Fig. 6A, the forward-sweeping peak current density of the PdPt@Pt/C catalyst for the MOR could be up to 2.93 A mg^{-1} Pt, which is about 2.85 and 3.91 times greater than that of the commercial Pt/C catalyst and the lab-prepared Pt/C catalyst, respectively. In addition, the onset and peak potentials of the PdPt@Pt/C catalyst (0.24 V) are 60 mV lower than that of the Pt/C catalyst (0.30 V). The peak potential for the reaction on the PdPt@Pt/C catalyst is 65 mV more negative than that on the commercial Tanaka Pt/C catalyst, indicating the enhanced electrode kinetics. This superior performance may be attributable to both the better dispersion of platinum

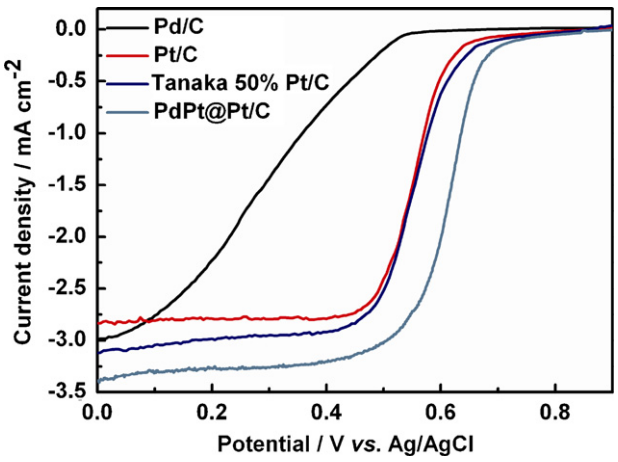

Fig. 7. Polarization curves of Pt/C, Pd/C, PdPt@Pt/C, and Tanaka 50% Pt/C catalysts in 0.5 M H_2SO_4 solution saturated with pure oxygen at a scan rate of 5 mV s^{-1} and a rotation speed of 1600 rpm.

on the PtPd core and the strong interaction between the outer Pt shell and the inner PtPd core.

The ratio of peak currents associated with the anodic peaks in forward (I_f) and reverse (I_b) is generally used to characterize the electrocatalytic activity of a catalyst for intermediates generated during the oxidation of methanol; for PdPt@Pt/C, the value of I_f/I_b was 1.04, which is much larger than that of the Tanaka catalyst (0.71) and the prepared Pt/C catalyst (0.75). This is a very significant and exciting result, as it indicates that the PdPt@Pt/C catalyst shows much better catalytic activity than pure platinum catalysts and yields fewer intermediates during anodic methanol oxidation. The remarkably high mass-specific oxidation current for the methanol oxidation reaction and good tolerance of CO_{ads} on the PdPt@Pt/C catalyst as compared to that of conventional Pt/C electrocatalysts indicates a more effective mechanism for promoting CO_{ads} removal, beyond the general theory of bifunctional catalysts. This is for three main reasons. First, the oxidative removal of CO_{ads} on the Pt shell is greatly accelerated by the availability of a large number of active oxygen-containing species on the underlying Pd core. The O 1s/C 1s atom ratio of PdPt@Pt/C is 0.13, while in both Pt/C and PtPd/C it is 0.10 according to the XPS results of Fig. 2A and B, indicating a higher density of surface function groups for the former, which is beneficial for the oxidation of methanol intermediates [15]. The other two reasons are associated with the high utilization rate of Pt and the interaction between the outer Pt shell and the inner Pd core.

Fig. 6B compares the activities of PtRu/C and PdPt@Pt/C catalysts. It is interesting that the PdPt@Pt/C showed higher activity, but PtRu/C ratio of I_f/I_b is high, up to 1.54, 50% higher than that of PtPd@Pt/C. This finding again confirms that the high I_f/I_b ratio of PtPd@Pt/C resulted from palladium.

As shown in Fig. 7, PtPd@Pt/C also showed higher activity than Pt/C towards oxygen reduction, even though the particle size of the pure platinum catalyst is smaller than that of the PdPt@Pt/C catalyst. We are continuing our intensive research and will be reporting the results soon.

3.3. Single-cell test

The performance of two MEAs prepared with PdPt@Pt/C and Tanaka 50 wt% Pt/C as the anode catalysts was compared, as shown in Fig. 8, in a hydrogen-air single cell at 0.65 V cell voltage; the current density of the MEA with PdPt@Pt/C as the anode catalyst was 544 mA cm^{-2}, over 80% higher than that of the MEA prepared with Tanaka 50 wt% Pt/C and operating under the same conditions.

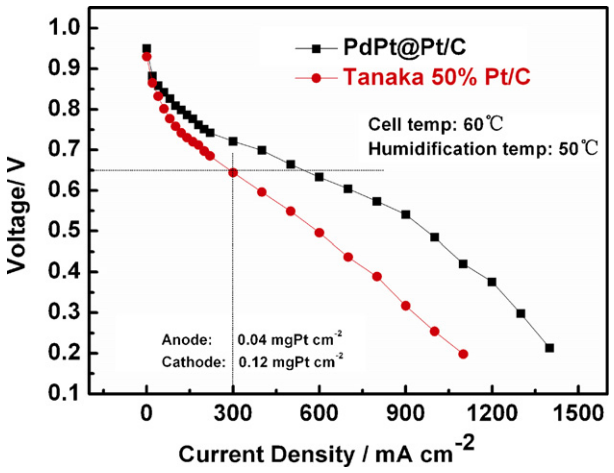

Fig. 8. Performances of MEAs prepared with PdPt@Pt/C and Tanaka 50 wt% Pt/C as the anode catalysts, in a H_2/air single cell.

4. Conclusions

In conclusion, a core–shell structured PdPt@Pt/C catalyst was prepared by a novel two-step colloidal approach. The core–shell structure of the catalyst was investigated by TEM, XPS, and UPDH, and the results revealed evidence of the catalyst having core–shell structure characteristics. By using PdPt alloy instead of Pd as the core, the problem of Pd aggregation was effectively avoided, resulting in a high dispersion of the active components. The catalyst showed extremely high activity for methanol oxidation and oxygen reduction, as well as higher tolerance to poisoning by intermediates generated in the process of anodic methanol oxidation than did the Pt/C catalyst. For anodic oxidation of methanol, the ratio of I_f/I_b could be as high as 1.04, making PdPt@Pt/C a promising and competitive low-Pt catalyst for PEMFC or DMFC applications.

Acknowledgments

We would like to thank the National Scientific Foundation of China (NSFC Project Nos. 20673040, 20876062) and the Guangdong Provincial Scientific Foundation (Project No. 36055) for financial support of this work.

References

[1] R. Borup, J. Meyers, B. Pivovar, Y.S. Kim, R. Mukundan, N. Garland, D. Myers, M. Wilson, F. Garzon, D. Wood, P. Zelenay, K. More, K. Stroh, T. Zawodzinski, J. Boncella, J.E. McGrath, M. Inaba, K. Miyatake, M. Hori, K. Ota, Z. Ogumi, S. Miyata, A. Nishikata, Z. Siroma, Y. Uchimoto, K. Yasuda, K.I. Kimijima, N. Norio Iwashita, Chem. Rev. 107 (2007) 3904–3951.
[2] S.J. Liao, K.A. Holmes, H. Tsaprailis, V.I. Birss, J. Am. Chem. Soc. 128 (2006) 3504–3505.
[3] J.L. Fernández, V. Raghuveer, A. Manthiram, J.A. Bard, J. Am. Chem. Soc. 127 (2005) 13100–13101.
[4] M.H. Shao, K. Sasaki, R.R. Adzic, J. Am. Chem. Soc. 128 (2006) 3526–3527.
[5] K.B. Jena, R.C. Raj, Langmuir 23 (2007) 4064–4070.
[6] R. Bashyam, P. Zelenay, Nature 443 (2006) 63–66.
[7] K. Lee, L. Zhang, J.J. Zhang, Electrochem. Commun. 9 (2007) 1704–1708.
[8] X. Wang, Y.W. Tang, Y. Gao, T.H. Lu, J. Power Sources 175 (2008) 784–788.
[9] B.K. Lim, M.J. Jiang, P.H.C. Camargo, E.C. Cho, J. Tao, X.M. Lu, Y.M. Zhu, Y.N. Xia, Science 324 (2009) 1302–1305.
[10] R.R. Adzic, J. Am. Chem. Soc. 127 (2005) 12480–12481.
[11] M.B. Vukmirovic, J. Zhang, K. Sasaki, A.U. Nilekar, F. Uribe, M. Mavrikakis, R.R. Adzic, Electrochim. Acta 52 (2007) 2257–2263.
[12] N. Kristian, X. Wang, Electrochem. Commun. 10 (2008) 12–15.
[13] W.J. Zhou, J.Y. Lee, Electrochem. Commun. 9 (2007) 1725–1729.
[14] J. Luo, L.Y. Wang, D. Mott, P.N. Njoki, Y. Lin, T. He, Z.C. Xu, B.N. Wanjana, I. Im, S. Lim, C.J. Zhong, Adv. Mater. 20 (2008) 4342–4347.
[15] H. Wang, C.W. Xu, F.L. Cheng, M. Zhang, S.Y. Wang, S.P. Jiang, Electrochem. Commun. 10 (2008) 1575–1578.